

# Zeosil Nanoslabs: Building Blocks in $n\text{Pr}_4\text{N}^+$ -Mediated Synthesis of MFI Zeolite\*\*

Christine E. A. Kirschhock, Véronique Buschmann, Sebastien Kremer, Raman Ravishankar, Christophe J. Y. Houssin, Barbara L. Mojet, Rutger A. van Santen, Piet J. Grobet, Pierre A. Jacobs, and Johan A. Martens\*

The tetrapropylammonium (TPA)-ion-mediated formation of MFI-type zeolite from monomeric and polymeric silica sources has been studied. A similar mechanism involving self-organization of identical nanoscopic zeolite particles was observed independent of silicon source. Transmission electron microscopy (TEM) and small-angle X-ray scattering (SAXS) studies revealed the quantitative formation of rectangular, nanometer-sized slabs from silica sources by the reaction with an aqueous solution of TPA hydroxide. Zeosil nanoslabs with dimensions of  $2.7 \times 1.0 \times 1.3$ ,  $4 \times 2 \times 1.3$ ,  $4 \times 4 \times 1.3$ , and  $8 \times 8 \times 1.3 \text{ nm}^3$  result from the self-assembly of 2, 6, 12, and 48 TPA-containing precursors, respectively. Zeosil nanoslab surfaces are provided with alkyl pins and silicate framework holes. These nanoslabs combine to form tablets and MFI-type zeolite crystals.

Application of the hydrothermal gel method for zeolite synthesis has led to the large diversity of synthetic zeolite materials known today.<sup>[1]</sup> Structure specificity is obtained by using organic structure-directing agents. Whereas it was recognized early that silicate-based crystals nucleate and grow from silicate oligomers,<sup>[2]</sup> progress in identification of precursors and their polycondensation processes was hindered by the presence of gel. The possibility of growing zeolites from “clear solution” rendered the processes experimentally more accessible,<sup>[3]</sup> and led to the present discovery of zeosil nanoslabs, which we identified as building blocks in the TPA-ion-mediated synthesis of zeolite MFI.

The zeosil silicalite-1 with a silicon dioxide framework and MFI framework topology,<sup>[4]</sup> crystallizes by heating a “clear solution” prepared from tetraethylorthosilicate (TEOS), tetrapropylammonium hydroxide (TPAOH), and water.<sup>[5]</sup> In the “clear solutions” studied in this work, all silicon was incorporated in nanosized particles.<sup>[6]</sup> Clear solution obtained from the hydrolysis of TEOS at  $20^\circ\text{C}$  in aqueous TPAOH solution<sup>[7]</sup> was spread on a grid for TEM studies. By taking all

necessary precautions,<sup>[8]</sup> we managed to observe a large number of nanosized particles (Figure 1 a). They were conglomerated and embedded in an organic matrix, which stemmed from TPA. The particles survived only a few seconds

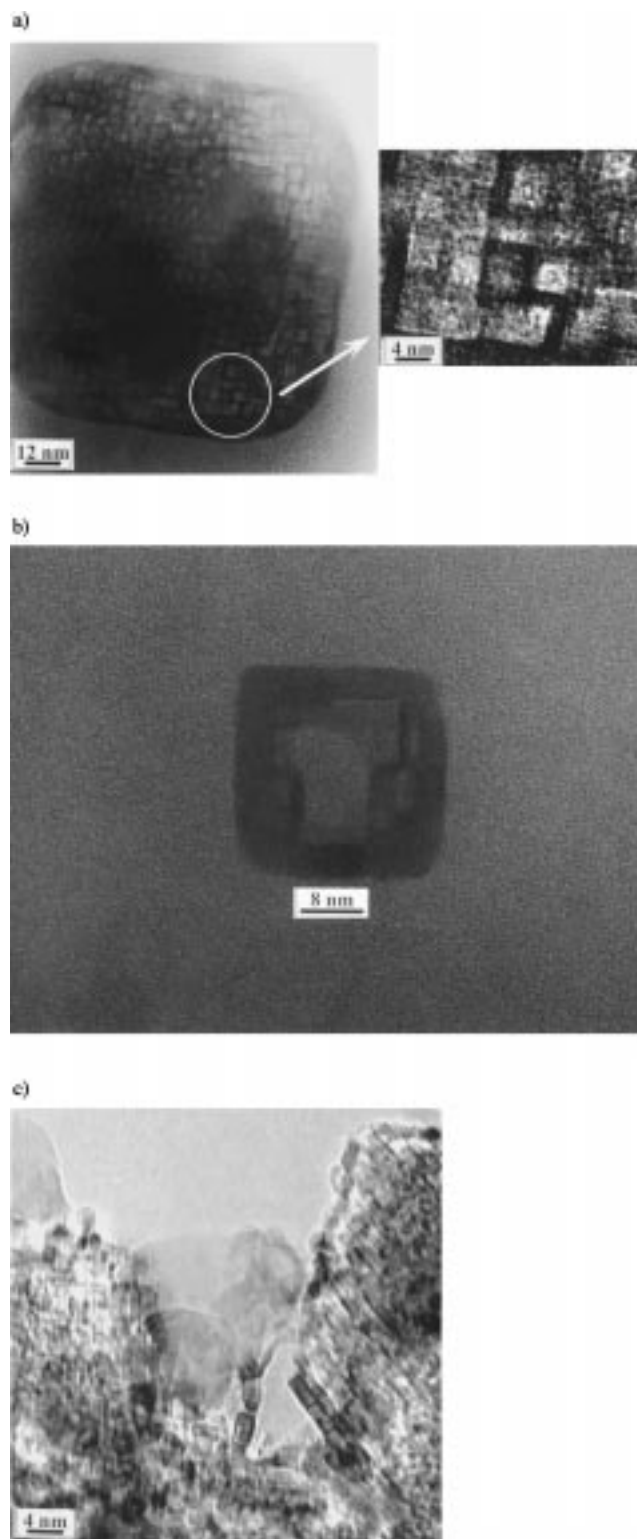


Figure 1. a) TEM images of nanoslabs **1**, prepared from the TEOS/TPAOH/water system;<sup>[7]</sup> b) occasionally observed larger block in nanoslab **1** sample; c) nanoslabs **3**, prepared from silicic acid, TPAOH, and NaOH.<sup>[11]</sup> Observations made with Philips CM200 TEM (200 kV, point resolution 0.19 nm) and a JEOL JEM3010 (300 kV, point resolution 0.17 nm) instruments equipped with a Gatan GIF200 electron energy loss spectrometer.

[\*] Prof. J. A. Martens, Dr. C. E. A. Kirschhock, S. Kremer, Dr. R. Ravishankar, Prof. P. J. Grobet, Prof. P. A. Jacobs  
Department of Interface Chemistry, K.U. Leuven  
Kasteelpark Arenberg 23, 3001 Leuven (Belgium)  
Fax: (+32)16-321998  
E-mail: johan.martens@agr.kuleuven.ac.be

Dr. V. Buschmann  
Materials Science Department  
Technische Universität Darmstadt  
Darmstadt (Germany)

C. J. Y. Houssin, Dr. B. L. Mojet, Prof. R. A. van Santen  
Schuit Institute of Catalysis

Eindhoven University of Technology, Eindhoven (The Netherlands)

[\*\*] C.E.A.K., J.A.M., and P.A.J. acknowledge the Belgian Government for sponsoring in the frame of IUAP-PAI program. J.A.M. and P.A.J. acknowledge FWO Vlaanderen for a research grant.

in the electron beam. This and their movements hindered the recording of diffraction patterns. The average in-plane dimensions of individual particles (nanoslabs **1**) were about  $4 \times 4 \text{ nm}^2$ , with a thickness of about 1 nm as revealed by the dimensions of standing particles. Occasionally, larger blocks (Figure 1b) were observed which had in-plane dimensions corresponding to multiples of 4 nm, suggesting they were formed through sidewise coalescence of elementary nanoslabs **1** of dimensions  $4 \times 4 \text{ nm}^2$ .

The SAXS pattern of a suspension of nanoslab **1** is shown in Figure 2a. The asymmetric line shape reveals deviation from spherical particle morphology. For slabs measuring  $4 \times 4 \text{ nm}^2$ ,

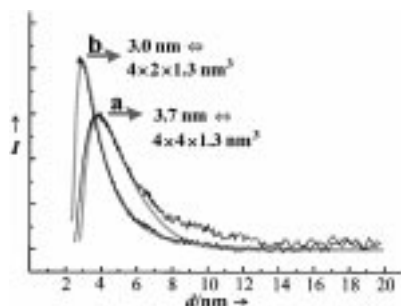


Figure 2. SAXS curves of suspensions of **1** (curve a) and **3** (curve b). Position and shape of measured intensities agree with simulated patterns (gray lines),<sup>[9]</sup> assuming uniform slablike bodies of dimensions  $4 \times 4 \times 1.3 \text{ nm}^3$  (curve a) and  $4 \times 2 \times 1.3 \text{ nm}^3$  (curve b). Measurements performed at the DUBBLE beamline (European Synchrotron Radiation Facility, Grenoble, France) by using a 2D gas-filled detector and a wavelength of 0.099 nm.

the observed characteristic length  $d$  of 3.7 nm corresponds to a thickness of 1.3 nm.<sup>[9]</sup> Thus the shape and position of the experimental scattering curve match with the theoretical scattering function for slabs measuring  $4 \times 4 \times 1.3 \text{ nm}^3$  (Figure 2a).<sup>[9]</sup> The SAXS study reveals the almost exclusive presence of a large number of unique and identical particles. The scattering intensity at  $d$  values larger than 6 nm, which is not accounted for by the theoretical curve, stems from the small amount of larger blocks also revealed by TEM (Figure 1b) and formed from nanoslab **1** by fusion. The thickness of 1.3 nm, derived from analysis of SAXS patterns, coincides with the range of characteristic step heights of  $1.2 \pm 0.3 \text{ nm}$  determined on evaporated suspensions by using atomic force microscopy.<sup>[10]</sup> The distribution of edge ( $Q^2$ ), surface ( $Q^3$ ), and bulk ( $Q^4$ ) silicon atoms, determined with  $^{29}\text{Si}$  MAS NMR spectroscopy, is also in agreement with dimensions of 1.3, 4, and 4 nm in the  $a$ ,  $b$ , and  $c$  crystallographic directions of silicalite-1, respectively.<sup>[10]</sup>

A suspension of nanoslab **1** was heated for 2 h at  $100^\circ\text{C}$ . The SAXS Porod plot (Figure 3) shows a region with negative slope of  $-2$  characteristic of flat surfaces having a characteristic length  $d$  of about 7.3 nm. This  $d$  value corresponds to bodies of  $8 \times 8 \times 1.3 \text{ nm}^3$ ,<sup>[9]</sup> designated as nanoplates **2**, obtained by systematic two-by-two sidewise joining of four nanoslabs **1**.

Industrial MFI-type zeolite crystallization processes start with silica rather than TEOS, and sodium hydroxide provides the necessary alkaline conditions. TEM studies of the product from room temperature digestion of silicic acid in an aqueous

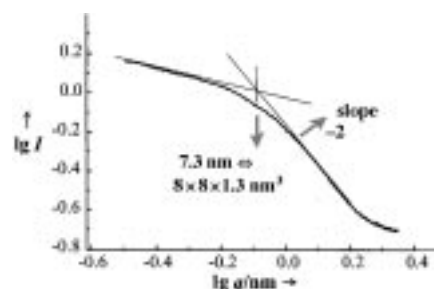


Figure 3. SAXS Porod plot of nanoplates **2**. Measurement conditions see legend to Figure 2.

solution of TPA and sodium hydroxide<sup>[11]</sup> revealed the occurrence of rectangular particles designated nanoslab **3** with in-plane dimensions of  $4 \times 2 \text{ nm}^2$  (Figure 1c). The SAXS pattern of this sample (Figure 2b) was again in excellent agreement with the theoretical scattering curve of uniform slab-shaped bodies. Introduction of the  $4 \times 2 \text{ nm}^2$  dimensions of nanoslab **3** derived from the TEM studies in the theoretical scattering expression revealed a thickness of 1.3 nm,<sup>[9]</sup> similar to those for **1** and **2** prepared from TEOS.

The polymerization of silica from TEOS proceeds over a bicyclic pentamer, a pentacyclic octamer, a tetracyclic undecamer, and finally the precursor **4**.<sup>[12]</sup> This precursor is unique to the MFI framework connectivity, occludes a TPA molecule, and measures  $1.3 \times 1.0 \times 1.3 \text{ nm}^3$ .<sup>[6, 12]</sup> This silica polymerization process is driven by creation of hydrophobic silica surfaces, which shield the propyl groups of the TPA ion from the aqueous solution.

An  $^{29}\text{Si}$  NMR spectrum recorded at an early stage of silicic acid digestion by TPAOH provided evidence for the occurrence of a bicyclic pentamer, a tetracyclic undecamer, and the precursor **4** (Figure 4a),<sup>[13]</sup> and the same silica polymerization sequence as with TEOS. The  $^{29}\text{Si}$  NMR signals were very weak and substantially broadened compared to those in the spectrum of precursor **4** in the TEOS system (Figure 4b) because the silicate species were not solution-borne but still adsorbed on remaining solid silica.  $^{29}\text{Si}$  NMR signals were absent after removal of the solids by filtration over a filter

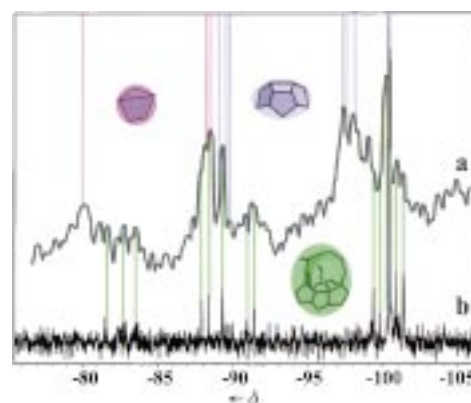


Figure 4.  $^{29}\text{Si}$  NMR spectrum at an early stage of silicic acid digestion (a). Chemical shifts of the bicyclic pentamer, the tetracyclic undecamer, and the precursor **4** taken from ref. [12] are indicated. For comparison, the  $^{29}\text{Si}$  NMR spectrum of precursor **4** in the TEOS system (b).<sup>[12]</sup> Spectra recorded on a Bruker AMX 300 MHz at  $0^\circ\text{C}$  using a pulse length of 4  $\mu\text{s}$  ( $45^\circ$  pulse), repeating time of 20 s,<sup>[12]</sup> and 2000 accumulations.

with a pore size of 100 nm. The presence of amorphous colloidal silica together with the oligomers was manifested in the broad underlying signals in the  $^{29}\text{Si}$  NMR spectrum (Figure 4a).

Additional evidence for formation of nanoslabs by self-assembly of precursor **4** irrespective of the silica source came from experiments with higher concentrations of TPAOH.<sup>[14]</sup> The products derived from TEOS and silicic acid exhibited a very similar scattering curve that can be simulated by the scattering of double precursor **5** with measurements of  $2.7 \times 1.0 \times 1.3 \text{ nm}^3$  (Figure 5).

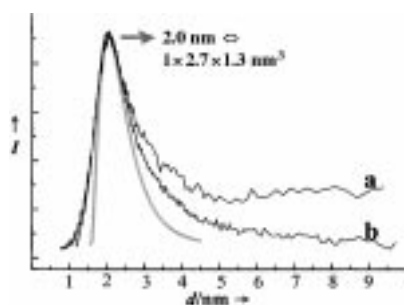


Figure 5. SAXS curves of clear solutions prepared from TEOS (a) and silicic acid (b) with an excess of TPAOH. The gray curve shows the simulation using the shape factor of a slab corresponding to two sidewise-linked precursors **4**. a) Data obtained on a Stoe Stadi P instrument,  $\text{Cu}_{\text{K}\alpha 1}$  radiation, and a position sensitive detector ( $5^\circ$ ); b) measured as described in legend to Figure 2.

The self-assembly of precursor **4** into specific nanoslabs depending on TPA and sodium concentration (Figure 6) reflects the peculiar colloidal properties of these organic–inorganic hybrid materials. At  $100^\circ\text{C}$ , suspended nanoplates **2** gradually form stacks which finally join sidewise to give the bulk MFI-type zeosil.<sup>[15]</sup> The stacked nanoplates are evident in the crystal morphology.<sup>[16]</sup>

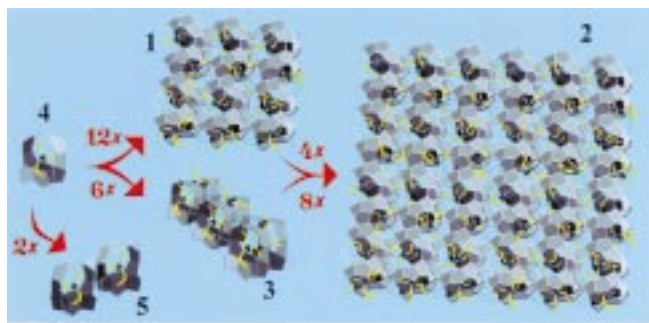


Figure 6. Schematic representation of the atomic structure of MFI-type zeosil nanoslabs **1**, nanoplate **2**, nanoslab **3**, their precursor **4**, and the double precursor **5**. The alkyl chains of TPA molecules are in yellow, nitrogen atoms in blue. The gray areas depict the silicate framework, at the corners of which are found silicon atoms, which are linked along the edges by oxygen atoms.

The present observation of nanoslabs in differently prepared suspensions suggests that the particles with equivalent diameters of 2.8–4.3 nm, which have been detected in MFI-type zeolite syntheses with dynamic light scattering, SAXS, and neutron scattering,<sup>[17]</sup> also belong to the nanoslab family.

This further supports the view that the formation and self-organization of nanoslabs are key steps in TPA-ion-mediated MFI synthesis. The observation and identification of zeosil nanoslabs can be exploited to modify the properties of zeolite-like products by manipulation of the aggregation conditions.

The surfaces of the nanoslabs are covered with pins and holes (Figure 6). Propyl groups of trapped TPA ions protruding out of the three faces of each nanoslab provide the pins, while the micropore openings on the opposite sides form the holes. At room temperature, a steric barrier caused by the propyl groups prevents the fusion of nanoslabs.<sup>[15]</sup> Even here there is already a strong tendency for self-organization, as revealed by the TEM photograph of the film formed by evaporation of the clear solution (Figure 1a). This self-organization can be directed to prepare organized physical bodies, monoliths, and liquid crystals. A concentrated suspension of nanoslabs exhibits schlieren patterns after ultrasonification. Transparent zeosil films with homogeneous thickness were prepared by spreading a suspension of nanoslab **1** onto a glass support and adding methanol after partial drying. Zeosil nanoslabs are versatile building blocks. By substituting TPAOH with TBAOH (tetrabutylammonium hydroxide), nanoslabs with MEL zeolite framework topology can be obtained.<sup>[6]</sup> Incorporation of titanium and aluminum atoms in MFI zeosil nanoslabs is possible as well.<sup>[18]</sup>

Received: November 17, 2000  
Revised: April 3, 2001 [Z16125]

- [1] R. M. Barrer, *Hydrothermal Chemistry of Zeolites*, Academic Press, London, **1982**.
- [2] “Zeolite Microporous Solids: Synthesis, Structure and Reactivity”: J. P. Gilson, *NATO ASI Ser. Ser. C* **1992**, 352, 511–529.
- [3] a) S. Ueda, N. Kageyama, H. Murata, M. Koizumi, S. Kobayashi, Y. Fujiwara, Y. Kyogoku, *J. Phys. Chem.* **1984**, 88, 2128–2131; b) “Zeolite Synthesis”: J. J. Keijsper, M. F. M. Post, *ACS Symp. Ser.* **1989**, 398, 28–48; c) C. C. J. Den Ouden, R. W. Thompson, *J. Colloid Interface Sci.* **1991**, 143, 77–84.
- [4] a) H. Gies, *Stud. Surf. Sci. Catal.* **1994**, 85, 295–325; b) E. M. Flanigen, J. M. Bennet, R. W. Grose, J. P. Cohen, R. L. Patton, R. M. Kirchner, J. V. Smith, *Nature* **1978**, 271, 512–516.
- [5] a) A. E. Persson, B. J. Schoeman, J. Sterte, J.-E. Otterstedt, *Zeolites* **1994**, 14, 557–567; b) P. P. E. A. De Moor, T. P. M. Beelen, R. A. van Santen, *J. Phys. Chem. B* **1999**, 103, 1639–1650; c) J. N. Watson, L. E. Iton, R. I. Keir, J. C. Thomas, T. L. Dowling, J. W. White, *J. Phys. Chem. B* **1997**, 101, 10094–10104.
- [6] C. E. A. Kirschhock, R. Ravishankar, L. Van Looveren, P. A. Jacobs, J. A. Martens, *J. Phys. Chem. B* **1999**, 103, 4972–4978.
- [7] The molar composition expressed in oxide ratios:  $(\text{TPA}_2\text{O})(\text{SiO}_2)_5(\text{H}_2\text{O})_{60}(\text{EtOH})_{20}$ .
- [8] Precautions: a defocused electron beam, rather low magnifications, and a video camera connected to the TEM-camera to monitor any possible change in time.
- [9] The mathematical expression for the scattering function of uniform isolated slabs is given in ref. [6]. The shape of the scattering function mirrors the distribution of possible trajectories through the body. The relation between the characteristic length  $d$  with maximum scattering intensity and the diagonal in space  $D$  of the slab is  $d = 0.64D$ .<sup>[6]</sup> The observed SAXS patterns agree much less with other particle shapes, like spheres.
- [10] R. Ravishankar, C. E. A. Kirschhock, P. P. Knops-Gerrits, E. J. P. Feijen, P. J. Grobet, P. Vanoppen, F. C. De Schryver, G. Miehle, H. Fuess, B. J. Schoeman, P. A. Jacobs, J. A. Martens, *J. Phys. Chem. B*, **1999**, 103, 4960–4964.

- [11] The molar composition of this mixture prepared from silicic acid, TPAOH, and NaOH:  $(\text{TPA}_2\text{O})(\text{SiO}_2)_4(\text{Na}_2\text{O})_{0.33}(\text{H}_2\text{O})_{47}$ .
- [12] C. E. A. Kirschhock, R. Ravishankar, P. J. Grobet, P. A. Jacobs, J. A. Martens, *J. Phys. Chem. B* **1999**, *103*, 4965–4971.
- [13] The molar composition of this mixture prepared from silicic acid and TPAOH:  $(\text{TPA}_2\text{O})(\text{SiO}_2)_4(\text{H}_2\text{O})_{47}$ ; the suspension was gently heated to 50 °C to initiate reaction.
- [14] The molar composition of the TEOS system:  $(\text{TPA}_2\text{O})(\text{SiO}_2)_{3.75}(\text{H}_2\text{O})_{30}(\text{EtOH})_{15}$ ; in the silicic acid system, the sample was the final product from the preparation of ref. [11].
- [15] C. E. A. Kirschhock, R. Ravishankar, P. A. Jacobs, J. A. Martens, *J. Phys. Chem. B* **1999**, *103*, 11 021–11 027.
- [16] R. Ravishankar, C. E. A. Kirschhock, B. J. Schoeman, P. Vanoppen, P. J. Grobet, S. Storck, W. F. Maier, J. A. Martens, F. C. De Schryver, P. A. Jacobs, *J. Phys. Chem. B* **1998**, *102*, 4588–4597.
- [17] a) J. N. Watson, A. S. Brown, L. E. Iton, J. W. White, *J. Chem. Soc. Faraday Trans.* **1998**, *94*, 2181–2186; b) S. L. Burkett, M. E. Davis, *J. Phys. Chem.* **1994**, *98*, 4647–4653; c) P. P. E. A. De Moor, T. P. M. Beelen, R. A. Van Santen, *Microporous Mater.* **1997**, *9*, 117–130; d) T. A. M. Twomey, M. Mackay, H. P. C. E. Kuipers, R. W. Thompson, *Zeolites* **1994**, *14*, 162–168; e) B. J. Schoeman, *Stud. Surf. Sci. Catal.* **1997**, *105*, 647–654.
- [18] R. Ravishankar, C. E. A. Kirschhock, B. J. Schoeman, D. De Vos, P. J. Grobet, P. A. Jacobs, J. A. Martens in *Proc. 12th Int. Zeolite Conf., Vol. III* (Eds.: M. M. J. Treacy, B. K. Marcus, M. E. Bisher, J. B. Higgins), Materials Research Society, Warrendale, **1999**, pp. 1825–1832.

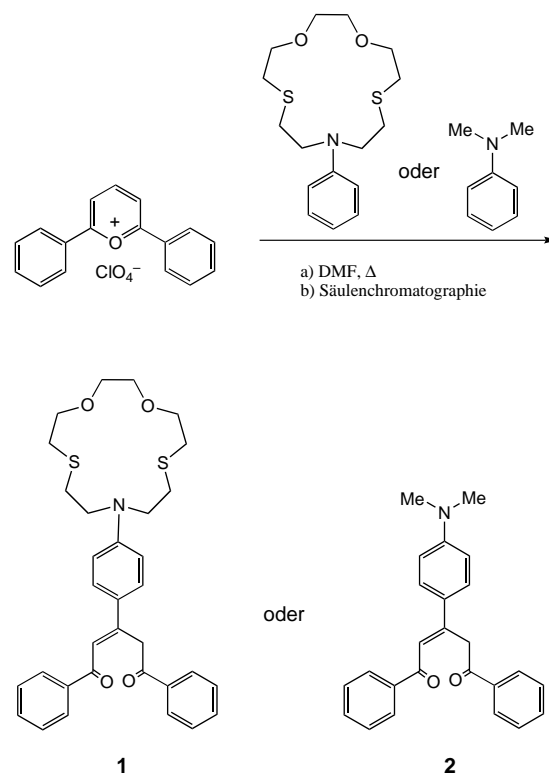
## A Colorimetric ATP Sensor Based on 1,3,5-Triaryl-2-en-1,5-diones\*\*

Félix Sancenón, Ana B. Descalzo, Ramón Martínez-Máñez,\* Miguel A. Miranda, and Juan Soto

The development of systems that are capable of sensing or recognizing and are based on supramolecular concepts is an area of current interest.<sup>[1]</sup> One of the most appealing approaches involves the construction of chromoionophores. Although such systems have been widely used for the analysis of metal cations,<sup>[2]</sup> chromogenic sensors for the “naked-eye” sensing of anions are not common;<sup>[3]</sup> this is especially the case in aqueous environments.<sup>[4]</sup>

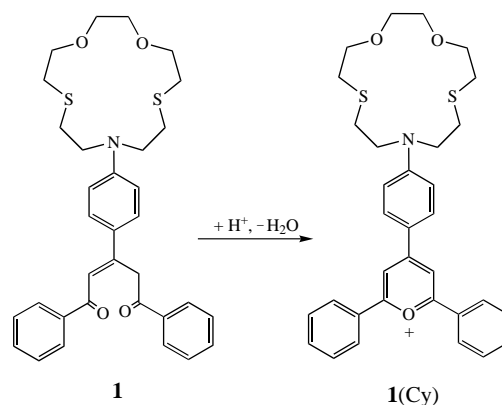
We report here the synthesis of 1,3,5-triaryl-2-en-1,5-dione derivatives and demonstrate their ability to act as colorimetric anion sensors. The new family of chromogenic reagents is easily obtained by condensation of the 2,6-diphenylpyrylium cation with N-functionalized anilines. For instance, the reaction of N-phenyl-1-aza-7,10-dioxo-4,13-dithiacyclopentadecane with 2,6-diphenylpyrylium gave the

1,3,5-triaryl-1,5-pentanedione derivative **1** after column chromatography (Scheme 1). The NMR (<sup>1</sup>H, <sup>13</sup>C) and mass spectra of **1** are consistent with the proposed formulation. The UV/Vis spectrum of **1** shows bands in the range of 200–300 nm along with a band centered at 380 nm, which is responsible for the pale yellow color of the receptor.



Scheme 1. Synthesis of the 1,3,5-triaryl-1,5-pentanedione derivatives **1** and **2**. The reaction is carried out in refluxing dimethylformamide (DMF) for 3 h, and subsequent column chromatography on alumina with  $\text{CH}_2\text{Cl}_2/\text{MeOH}$  (50/1 v/v) as eluent provides **1** (35 % yield) or **2** (50 % yield).

The 1,5-pentanedione system of **1** can be readily transformed into the corresponding pyrylium ion (Scheme 2):<sup>[5]</sup> Addition of nitric acid to solutions of **1** in 1,4-dioxane/water (70/30 v/v) caused a dramatic change in color from yellow to magenta. This change was accompanied by a new intense



Scheme 2. Transformation of the 1,5-pentanedione **1** into the pyrylium cation **1(Cy)**.

[\*] Dr. R. Martínez-Máñez, F. Sancenón, A. B. Descalzo, Prof. M. A. Miranda, Dr. J. Soto  
Departamento de Química  
Universidad Politécnica de Valencia  
Camino de Vera s/n, 46071 Valencia (Spain)  
Fax: (+34) 9-6-387-7349  
E-mail: rmaez@qim.upv.es

[\*\*] This research was supported by the Ministerio de Ciencia y Tecnología (proyecto PB98-1430-C02-02, 1FD97-0508-C03-01, and AMB99-0504-C02-01). F.S. also thanks the Ministerio de Educación y Cultura for a Doctoral Fellowship.